LANGMUIR

Subscriber access provided by La Trobe University Library

Article

Complex Thermodynamic Behavior of Single-Stranded Nucleic Acid Adsorption to Graphene Surfaces

Srivathsan V. Ranganathan, Ken Halvorsen, Chris A Myers, Neil M. Robertson, Mehmet Veysel Yigit, and Alan Austin Chen

Langmuir, **Just Accepted Manuscript** • DOI: 10.1021/acs.langmuir.6b00456 • Publication Date (Web): 24 May 2016

Downloaded from http://pubs.acs.org on June 1, 2016

Just Accepted

"Just Accepted" manuscripts have been peer-reviewed and accepted for publication. They are posted online prior to technical editing, formatting for publication and author proofing. The American Chemical Society provides "Just Accepted" as a free service to the research community to expedite the dissemination of scientific material as soon as possible after acceptance. "Just Accepted" manuscripts appear in full in PDF format accompanied by an HTML abstract. "Just Accepted" manuscripts have been fully peer reviewed, but should not be considered the official version of record. They are accessible to all readers and citable by the Digital Object Identifier (DOI®). "Just Accepted" is an optional service offered to authors. Therefore, the "Just Accepted" Web site may not include all articles that will be published in the journal. After a manuscript is technically edited and formatted, it will be removed from the "Just Accepted" Web site and published as an ASAP article. Note that technical editing may introduce minor changes to the manuscript text and/or graphics which could affect content, and all legal disclaimers and ethical guidelines that apply to the journal pertain. ACS cannot be held responsible for errors or consequences arising from the use of information contained in these "Just Accepted" manuscripts.

ACS Publications

Langmuir is published by the American Chemical Society. 1155 Sixteenth Street N.W., Washington, DC 20036

Published by American Chemical Society. Copyright © American Chemical Society. However, no copyright claim is made to original U.S. Government works, or works produced by employees of any Commonwealth realm Crown government in the course of their duties.

Complex thermodynamic behavior of single-stranded nucleic acid adsorption to graphene surfaces

Srivathsan V. Ranganathan[†], Ken Halvorsen[†], Chris A. Myers[‡], Neil M. Robertson[‡], Mehmet V. Yigit[†, ‡*] and Alan A. Chen[†, ‡, *]

‡Department of Chemistry,

University at Albany, State University of New York,

1400 Washington Avenue, Albany, New York 12222, United States

†The RNA Institute,

University at Albany, State University of New York,

1400 Washington Avenue, Albany, New York 12222, United States

*Correspondence:

Tel: (1) 518-437-4420

achen6@albany.edu and myigit@albany.edu

FootNote: KH and SVR equally contributed to the work.

Abstract:

In just over a decade since its discovery, research on graphene has exploded due to a number of potential applications in electronics, materials, and medicine. In its water-soluble form of graphene oxide, the material has shown promise as a biosensor due to its preferential absorption of single-stranded polynucleotides and fluorescence quenching properties. The rational design of these biosensors, however, requires an improved understanding of the binding thermodynamics and ultimately a predictive model of sequence-specific binding. Towards these goals, here we directly measured the binding of nucleosides and oligonucleotides to graphene oxide nanoparticles using Isothermal Titration Calorimetry (ITC), and used the results to develop molecular models of graphene-nucleic acid interactions. We found individual nucleosides binding with K_D values in sub-millimolar range with binding order of rG<rA<rC<dT<rU, while 5mer and 15mer oligonucleotides had markedly higher binding affinities in the range of micromolar and sub-micromolar K_D values, respectively. The molecular models developed here are calibrated to quantitatively reproduce the above-mentioned experimental results. For oligonucleotides, our model predicts complex binding features such as double stacked bases, and a decrease in the fraction of graphene stacked bases with increasing oligonucleotide length until plateauing beyond ~ 10-15 nucleotides. These experimental and computational results set the platform for informed design of graphene-based biosensors, further increasing their potential and application.

Keywords: graphene, nanoparticle, DNA, RNA, biosensors

Introduction

Since its discovery just over a decade ago, the two-dimensional carbon lattice known as graphene has sparked significant interest due to its unique features.[1,2] Due to its extraordinary electrical, thermal, and mechanical properties it has been used for a variety of applications ranging from constructing radar-absorbing surfaces for airplanes[3] to designing drug delivery or imaging vectors for *in vivo* animal studies.[4] The graphene itself has been primarily investigated for device engineering[5-7] while its water-soluble form, graphene oxide, has been utilized particularly for biosensor development.[8-10] The nanoscale graphene oxide (nGO) is highly dispersed and stable in aqueous solution. It has been used for a wide array of biological studies due to its highly useful and unique properties at the bio-nano interface.[11,12] Its interaction with single stranded nucleic acids has attracted significant attention for RNA and DNA detection,[13] biomedical and biological imaging, aptasensor designs and environmental monitoring.[14,15] nGO has a remarkable single stranded oligonucleotide adsorption capacity due to specific intermolecular interactions (aromatic stacking, van der Waals forces, hydrophobic interactions, and hydrogen bonding) between its planer honeycomb surface and nucleobases of the oligonucleotides.[16] nGO can bind reversibly to single stranded oligonucleotides, which can be released from the surface in the presence of complementary strands or oligo-binding target strands,[13,17-19] an extremely attractive feature for biosensing applications. However, an effective biosensor must avoid both false-positive and false-negative signals that would arise from probes that bind too weakly or strongly to the nGO surface prior to hybridizing with a target sequence. Therefore, we must first understand how the thermodynamics of ssDNA adsorption to nGO change as a function of both probe length and sequence composition before we can rationally engineer efficient nGO-based biosensors.

Prior computational work on this topic has primarily focused on nucleobase interaction with graphene in vacuum.[20] Although these studies have yielded valuable insights on the strength and nature of interactions in vacuum, a quantitative understanding of how these interactions are affected by aqueous solvent has remained poorly understood. While explicit-solvent simulations are ideally suited for characterizing interactions in the relevant aqueous environment, they

require the development of a force-field that accurately depicts graphene-nucleobase interactions. Lacking an accurate model, solvent is typically represented only implicitly[21,22] or excluded altogether in prior studies. In this work, we have systematically studied the interactions of single nucleosides and DNA molecules of differing lengths and sequences, adsorbing to a nGO surface in an aqueous environment, using complementary computational and experimental approaches. Using isothermal titration calorimetry (ITC), we measured dissociation constants for individual nucleosides as well as short oligonucleotides. This experimental binding data, combined with measurements from DFT calculations, were used to calibrate a molecular mechanics force-field for nucleic acid/nGO interactions, enabling detailed *in-silico* studies to probe ssDNA structure and interaction at graphene surfaces. Using our newly developed, experimentally calibrated molecular model, we uncover complex binding patterns for oligonucleotides to graphene that paves the way for improved design of graphene-based biosensors.

Materials and Methods

Materials. All DNA sequences (poly A, poly T, poly G, and poly C) were purchased from Integrated DNA Technologies (IDT), (Coralville, IA 52241, USA). All reagents were purchased from Sigma-Aldrich (St. Louis, MO 63103, USA) and used without further purification. RNAse-free water was used in preparation of all oligonucleotide solutions.

A carboxyl graphene oxide water dispersion was purchased from ACS Material (Medford, MA, USA) and sonicated 12 h before use to obtain a water-soluble nanosized graphene oxide (nGO) solution. The average particle size and zeta potential were determined to be 283.3 ± 15 nm and -23.7 ± 2.9 mV, respectively, using a Malvern Instruments Zetasizer Nano ZS. RNase-free water was used for the preparation of all solutions

Methods.

Preparation of oligonucleotide and nucleoside suspension:

Powder nucleosides were dissolved in deionized (DI) water and diluted to their working concentrations before use. Concentrations were measured by absorbance at 260nm on a Nanodrop spectrophotometer, using their extinction coefficients.[23] Adenosine, guanosine, and cytidine were all brought to within 1% of 1mM as determined by the mean of three replicate

measurements. Uridine and thymidine were brought to within 1% of 10mM. All nucleoside solutions were stored at 4˚C, with the exception of guanosine and deoxyguanosine, which were stored at room temperature due to their low solubility. Each of the five nucleosides was stored in the low binding tubes (Eppendorf) and all experiments were performed using these stocks. Oligonucleotides were purchased from IDT and diluted to 1mM in DI water.

Isothermal titration calorimetry (ITC) studies:

All ITC experiments were performed using the low volume Nano ITC (TA Instruments) at 25℃. The instrument was factory calibrated using $KHCO_3$-HCl titrations to determine the effective cell volume. The injection syringe was calibrated by mass of water.[24,25] Experiments consisted of titrating the relevant nucleoside or oligonucleotide into the nGO solution, typically with 2.5μL injections spaced 200 s apart with 350 rpm stirring. For uridine and thymidine, 5μL injection volumes were used due to the lower heat of injection. All experiments were performed using single "parent" stocks of nGO and reduced nano-graphene oxide particles. The OD value at 230 nm was used to normalize the amount of graphene for each experiment.

Integration of the heat curves was performed using the NanoAnalyze software (TA Instruments), with automated baseline construction, integrating from the injection start to 150-200 s post injection. The curves were individually fit with two state binding models with a constant baseline adjustment to account for the mixing enthalpy contribution. The first data point was excluded from analysis as is the convention, as was the last data point due to typically anomalous lower heat. For individual nucleosides, curve fitting was performed on the mean data from replicated experiments. For oligonucleotides with full binding curves, we performed unconstrained fitting to determine binding constants, enthalpies, and stoichiometries with errors determined using a bootstrapping statistical analysis built in to the NanoAnalyze software. Uncertainty in extinction coefficients of the polynucleotides[26] (which proportionately affect enthalpy and stoichiometry measurements with only minor effects on free energy) are not included in the error bars.

The upper and lower limits of the enthalpy for the constrained curve fitting were determined as follows. The lower limit of the enthalpy range for the nucleosides was conservatively chosen to be -27 kcal/mol based on *in silico* results of the most enthalpically favorable nucleobase-graphene interaction in vacuum[27]. The upper limit for the enthalpy was determined by experimental data of the largest normalized heat (in kcal/mol) from the first injection of each of

the nucleosides. Much of this data came from preliminary experiments in which various concentrations of nGO and nucleoside were tested before settling on final experimental parameters. For a few experiments, our upper limit from this experimental data was too high, and for those cases we reduced the upper limit enthalpy until the fit was acceptable.

Quantum Chemical Calculations:

All quantum calculations were performed at the B3LYP-D3 level of theory using the Q-Chem software package[28]. The system consisted of the nucleobase molecule in a plane parallel to a fragment of the graphene sheet (70 atoms) in vacuum. The nucleobase was geometry optimized in isolation, and then the distance between the base and the graphene plane was varied to measure interactions energies as a function of distance. Dunning's correlation consistent cc-pVTZ basis set was used and the counterpoise correction was employed to minimize basis set superposition error (BSSE). Prior work has demonstrated the effectiveness of Grimme's DFT-D3 dispersion-correction combined with the commonly employed B3LYP density functional to accurately describe the energetics of non-covalent stacking interactions between aromatic complexes including nucleobases [29,30]

Molecular Dynamics (MD) simulations:

System: Our MD simulation systems consisted of a graphene sheet and a nucleic acid species (a nucleoside or an oligonucleotide) in the presence of water. The graphene sheet was constructed by placing carbon atoms in a hexagonal honeycomb lattice with a lattice spacing of 0.142 nm, and was not allowed to move during the course of the simulations. The XY dimensions of the box were chosen such that the graphene sheet is infinitely periodic in those dimensions. For the single nucleoside system, the XY dimensions are 4.175 x 4.254 nm^2, and for the largest system studied (20mer) 15.227 x 15.314 nm^2 box was used. The thickness of the water layer on graphene, ~ 4 nm (containing about 2500 to 30,000 molecules depending on the system size). Other than single nucleosides (rA, rG, rC & rU) and homo-pentanucleotides (A_5, C_5 and T_5), we also studied longer homo- and mixed sequence oligomers. We studied a poly-A sequence of 15 bases, and repeats of $(ATGCA)_n$, where n = 1, 2, 3 and 4.

Methodology: All MD simulations were performed using the Gromacs-4.6.3 package.[31] Leapfrog algorithm with a 2 fs time-step was used to integrate the equations of motion and

propagate the trajectory. All systems were studied in an NVT ensemble using V-rescale thermostat to maintain the temperature constant through the course of the simulation.[32] The long-ranged electrostatic interactions were calculated using particle mesh Ewald (PME)[33] algorithm with a real space cut-off of 1.2 nm. LJ interactions were also truncated at 1.2 nm. TIP3P model[34] was used represent the water molecules, and LINCS[35] algorithm was used to constrain the motion of hydrogen atoms bonded to heavy atoms. The oligos (5mers, 10mer, 15mer and 20mer) were simulated for 1 microsecond each, which consisted of 10 independent runs started from different initial conformations. The different initial conformations were obtained from a high temperature (1000K) simulation of the oligo in vacuum. In addition to conventional equilibrium MD simulations, we also performed umbrella sampling (US) and non-equilibrium pulling simulations to calculate binding free-energies of single nucleosides and off-rates of single nucleosides and short oligos, respectively. For the US simulations, we used 7 equally spaced windows in the short-range (between r_0 = 0.3 and 1.0 nm), and 5 equally spaced windows in the longer range (between r_0 = 1.0 and 1.6 nm), where r_0 is the graphene-nucleoside separation. A harmonic potential of $0.5k(r-r_0)^2$ was used to constrain the nucleoside-graphene distance in the vicinity of r_0. The force-constant (k) was varied systematically to get good overlap in the PMF, and are listed in **Table S5**. WHAM[36] method was used to unbias the distributions from US simulations to get underlying free-energy curves. Pulling simulations of single nucleosides and 5mers were done at constant force (40, 80 and 160 pN) and the reported off-rates are averages from 50 independent unbinding events.

Results and Discussion

The goal of this study is to develop a detailed thermodynamic model for nucleobase adsorption to nGO surfaces based on experimentally determined binding affinities. To this end, we first performed isothermal titration calorimetry (ITC) experiments to measure the energetics of graphene-nucleoside interactions (**Figure 1a, 1b,** and **Figure S1**). An ideal ITC experiment of a two state binding interaction will produce a sigmoidal curve with the midpoint indicating stoichiometry, the slope of the transition indicating K_D, and the height of the transition indicating enthalpy. Achieving these ideal conditions, however, requires use of titrant and titrand concentrations that are significantly higher than K_D, which cannot always be achieved due to solubility limits. Consistent with previous work[21], titration curves for individual nucleosides did

not show an inflection point, suggesting that nucleosides are in molar excess of the "binding sites" on the nGO. However, these incomplete curves can still yield important information about the binding constants. To determine binding constants, we fit the results with a two state binding model while constraining the enthalpy parameter to realistic values for each nucleoside to avoid degeneracy between enthalpy and stoichiometry in the fitting (see Methods). From this analysis, we determined upper and lower limits of the association constant and ΔG for each nucleoside (**Figure 1C**). It is worth noting that the association constant determined from the fit is only weakly dependent on the set enthalpy (**Figure 1C, inset**), which allows good estimates of binding free-energies even without complete knowledge of the binding enthalpy and the molar concentration of graphene binding sites. The association constants are in the order of rG>rA>rC>dT>rU, with slight overlap between rA and rC ranges and rU and dT ranges, indicating some uncertainty. Comparing the heat of the first injections (**Figure S1**) suggests that binding enthalpies follow the trend rC<rA<rG<dT<rU. Prior work, including both isothermal titration calorimetry (ITC)[21] and *in-silico* studies[27], have qualitatively demonstrated that the adsorption affinity of nucleobases to nGO follow the trend: G>A>C>T. Although the prior ITC experiments[21] measured the nucleoside-graphene interactions in an aqueous environment, the free energies or binding constants were not ascertained due to experimental uncertainties, which were addressed in this work. Additional experiments suggest that ribonucleosides and deoxyribonucleosides interact similarly with nGO particles (**Figure S1 and Table S1**), and that reduced graphene oxide (r-nGO) particles and nGO particles bind nucleosides with the same qualitative behavior and only minor quantitative differences (**Figures S1, S2; Tables S1, S2**), indicating that the oxidation state of graphene plays a minor role in nucleoside binding. This observation is consistent with the binding mode known to be dominated by pi-pi aromatic stacking interactions.

Next we measured the binding of DNA oligonucleotides with nGO particles. Here we obtained several complete binding curves (for AAAAA (A_5), C_5, and AGCTA) due to the increased binding affinities (**Figures 2a, 2b, and S3**), and a partial binding curve for T_5. We were not able to obtain binding data for G_5, which was anticipated due to the strong noncovalent interaction of G-bases with each other in G-rich sequences. We find that association constants for A_5 and C_5 that were ~40 to ~60 times higher than those of the individual nucleosides, with enthalpies in the range of -30 to -37 kcal/mol, suggesting that some but not all bases have

stacking interactions with the surface. Of the oligonucleotides for which data was obtained, the order in association constants is C_5~A_5>AGCTA>T_5, and the order in enthalpies is AGCTA~C_5<A_5 using incomplete data for T_5 due to the partial binding curve (**Figure 2c**). However, the enthalpy for T_5 can be inferred to be between -4 and -11 kcal/mol, if we assume that the stoichiometry for T_5 binding is similar to other oligonucleotides. The binding affinity of a longer poly-A oligomer with 15 bases showed another order of magnitude increase in binding affinity compared to its 5mer counterpart. The breakdown of the free-energy of binding of the oligos reveals huge enthalpy-entropy compensation with favorable enthalpic and unfavorable entropic contributions. In comparing the enthalpies of oligonucleotides with nucleosides, it can be seen that the enthalpy is sub-additive as multiple nucleosides are added together into oligonucleotides. Based on the approximate stoichiometry determined from these experiments (~0.1 for our assigned nGO concentrations), we can deduce that there are ~10 μM of binding sites in a ~100 μg/mL solution. Given a specific surface area of graphene on the order of ~ 10^{-4} $m^2/\mu g$[37], we obtain on the order of 1 nucleoside binding site per square nanometer, which suggests almost complete surface coverage.

Explicit-solvent molecular dynamics simulations are ideally suited to account for the detailed role of the aqueous solvent in nucleobase-nGO adsorption. Although there are a variety of molecular mechanics models for describing DNA and graphene separately, to our knowledge no existing force-field has been calibrated to reproduce actual experimental measurements of nucleobase-nGO interactions. Armed with the ITC data for validation, we developed parameters to accurately capture nucleic acid-graphene interactions in water. By performing molecular dynamics simulations of nucleosides at a graphene-water interface (**Figure 3**), we determined distance dependent potentials of mean force (PMF) between the nucleosides and graphene in water. The global minimum in all the curves is at ~0.4 nm, where the nucleosides are in contact with the graphene surface, as seen in **Figure 3b**. We first tested the existing, unmodified AMBER99 force-field parameters[38] to test its accuracy in representing nucleoside-graphene interactions. The PMFs are qualitatively similar amongst all four nucleosides, with their binding free-energies at the contact minima following the order rG<rA<rU<rC. Adsorption free energies calculated using the unmodified AMBER99 parameters were in the range of -11 to -16 kcal/mol (**Figure 3c and Supplemental note 1**). While the trend in binding free-energies is in agreement with previous studies,[21] the magnitudes are significantly different compared to the results from

ITC experiments (**Figure 1**). Specifically, the predicted binding free energies are roughly twice the experimentally measured values, amounting to several orders of magnitude difference in equilibrium constants. This discrepancy is not surprising in light of previous work showing that AMBER99 parameters over-stabilize stacking interactions, leading to artificially long-lived compaction of dinucleotides in MD simulations.[39] Given that the graphene-based biosensors rely upon the relative propensity of nucleic acids to hybridize compared to their binding affinities to the nGO surface, it is important that the models quantitatively reproduce the binding free-energies measured using ITC.

In addressing these discrepancies, we tested the Chen and Garcia parameters which were specifically parameterized to reproduce experimentally measured dinucleotide stacking propensities[39]. As shown in **Figure 3c**, Chen-Garcia parameters came noticeably closer to reproducing experimental values but still overestimated the stacking, which is not unexpected given the substantially larger stacking surface presented by graphene compared to a nucleobase. To improve the model, we performed a scaling of the Lennard-Jones (LJ) parameters based on both theoretical and experimental constraints. Informed by quantum calculations employing dispersion corrected DFT, we adjusted the atomic sizes (σ) to reproduce the repulsive part of LJ interactions (**Figure S4**). We then rescaled the interaction strength parameter (ε), to capture the correct experimentally determined binding free-energies. These recalibrated parameters (tabulated in **Table S4**) produced binding free-energies that are in close quantitative agreement with experimental measurements. Furthermore, similar to experiments the calibrated model predicts that binding is dominated by enthalpy (**Figure S5**). This enthalpy dominated binding is largely expected due to the direct pi-pi stacking interactions between nucleosides and graphene.

To further validate the model, we made predictions on the behavior of oligonucleotides at the graphene-water interface. Since direct evaluation of association constants or binding free-energies of oligonucleotide-graphene interaction was not computationally feasible, we performed pulling simulations to determine dissociation rates under applied force (**Figures S6**). These dissociation rates serve as a good measure to compare relative binding affinities, and we found good qualitative agreement with the experimental results. Specifically, we found the same trend in binding affinities among the oligos ($A_5 \sim C_5 > ATGCA > U_5$) as well as near-quantitative agreement (in the same order of magnitude) among the predicted and measured change in

binding free-energy (ΔΔG) values between single nucleosides and 5-mer oligonucleotides (**Figure S6**). The 1-2 order(s) of magnitude increase in the association constants for the 5mer oligos compared to the single nucleosides was reproduced in their respective dissociation rates calculated using the pulling simulations.

After validating the model, we performed extensive MD simulations of various length oligonucleotides at the graphene water interface (**Figure 4**). These simulations elucidated several structural complexities in oligonucleotide-graphene interactions. First, simulations of 5-mer oligonucleotides shows that, on an average, only 3 to 3.5 bases are predicted to be stacked on the graphene (**Figure 4c**) (A distance cut-off of 0.4 nm from the center of the base is used to identify the stacked configurations). This observation is consistent with the less than additive enthalpies experimentally observed, and suggests that simultaneously stacking all bases along the graphene surface is entropically unfavorable. Interestingly, both 5mer and 15mer poly-A (A_5 and A_{15}) oligos show significantly less stacking to graphene compared to the other oligos even though adenine has the highest stacking enthalpy at the level of an isolated nucleobase. Poly-A is known for its increased propensity for intra-strand stacking interactions, which effectively can sequester bases from interacting with the graphene surface. The non-linearity in the percentage of bases stacked with oligomer length is evident for the mixed sequences, as well as the poly-A oligomer. It is interesting to note that the percentage of bases stacked decreased from roughly 60% to 50% going from A_5 to A_{15}. This decrease amounts to just over a two-fold increase in the number of bases stacked (3.1 to 7.5), while there is a three-fold increase in oligomer length. The nearly two-fold increase in the measured enthalpy of binding between A_5 and A_{15} (**Figure 2c** & **Table S3**) is in good agreement with the simulations, which predict a sub-additive increase in base stacking in the poly-A sequences studied. For the mixed sequences, as the oligonucleotide length increases from 5 to 20 nt, the model predicts a non-linear decrease in the fraction of stacked bases (**Figure 4b**), eventually plateauing around 60% between 10 and 15 nucleotides. This plateau suggests a certain length scale (10 to 15 nt), above which the fraction bound to graphene becomes additive, which is consistent with experimentally determined binding constants of oligos (5, 10 and 20mer) reported by He et al.[40] While the binding of nucleic acids to graphene in the short length scale (from 1 to 5 nt) is non-additive and anti-cooperative, at the longer length scale (< 10 nt) it becomes additive. The additivity in the longer length scale may result from formation of sub-structures with stacks and loops which get repeated with increasing number of bases.

This behavior raises the interesting question of what happens to the bases that are not involved in direct graphene stacking. It can be seen (**Figure 4a & 4d**) that a significant fraction of these are multiply stacked (i.e. stacked on top of a graphene-stacked base), while the remainder are largely exposed to solution. Density profiles of the nucleobase atoms at the graphene surface shown in **Figure S7** clearly highlight the location of first and second layer stacks. The molecular structure of the oligos at the graphene surface provide valuable insights into the mechanism of desorption of nucleic acid oligos from graphene by complimentary DNA (cDNA), which is crucial for the efficient design of graphene based biosensors. It has been previously suggested that the hybridization of DNA-cDNA may occur either at the nGO surface or in solution depending on the concentration of nGO, the relative binding affinities of the DNA strands to nGO, and the extent of base complementarity between the DNA strands. In recent work by Liu et al.[41], it is suggested that probe strands, like poly-T DNA, are first displaced from the nGO surface by the complementary strand (poly-A), and only then undergo hybridization in solution. However, Park et al.[42] have shown that at high concentrations of nGO, where desorption of probe DNA is specific to introduction of cDNA, hybridization likely occurs at the nGO surface. In this context, the "super-stacked" (double- and triple-stacked) conformations observed here potentially reconcile both observations, as they may act as nucleation sites that enable rapid duplex formation and concomitant desorption of the duplex from the graphene surface. In ongoing work, the model presented here is being utilized to simulate duplex formation at nGO surface to gain a molecular understanding of the graphene desorption process for natural and chemically modified nucleic acids. It is anticipated these advances will enable the rational design of highly sensitive and robust graphene based biosensors.

Conclusion

Understanding the interaction between nucleobases and graphene surface is essential for developing efficient graphene-based biosensors, nanotools for delivery of anti-sense oligonucleotides for cancer theranostics and graphene-based nanopores for DNA sequencing. The work presented here enables molecular modeling of nucleic acid at graphene surfaces through an experimentally calibrated set of force-field parameters. These parameters recapitulate the observed non-additivity in the binding of oligonucleotides at the short lengthscale (1-5mer), and were further employed to study oligonucleotide-graphene adsorption as a function of oligo length. The simulations of oligonucleotides bound to graphene revealed that nearly 40% of bases

end up multiply stacked or solvent-exposed configurations. Our results also predict additivity in stacking of bases at the longer length scales, consistent with previously published experimental results. However, the electrostatic interactions arising from the charged groups on the nGO surface, which can become significant for longer oligomer (>10 bases) binding are not addressed in the current model. Further, while we find that at the single nucleoside/nucleotide level salt affects are minimal on graphene binding (**Figure S8**), the effects of salt have shown to be important for binding of longer oligomers.[43] The salt affects may arise through screening and bridging of backbone-backbone and backbone-surface interactions, respectively, which is currently being explored through experimental and simulation studies. Overall, this work lays a platform for modeling and simulations of nucleic-acid species at graphene surfaces towards design of graphene based biosensors, and also serves as a paradigm for developing experimentally calibrated molecular models for simulation of biomolecules.

Author Contributions

SVR designed, performed, and analyzed molecular simulations. KH designed, performed, and analyzed ITC experiments. CAM assisted with DFT calculations. NMR prepared graphene nanoparticles. MVY and AAC conceived of the study and designed research. SVR, KH, MVY, and AAC wrote the paper. SVR, KH equally contributed to the work. AAC and MVY are the corresponding authors.

Acknowledgements

We thank Ashley Colvin and Nicolas Peterson for helping with preliminary simulations for this work. We also thank Drs. Paul Agris, Maria Basanta Sanchez and Sweta Vangaveti for numerous insightful discussions. This work was supported by a research grant from the PhRMA Foundation (A.A.C.) and by University at Albany start-up funds (A.A.C & M.V.Y.). This work used the computing resources of the Extreme Science and Engineering Discovery Environment (XSEDE), which is supported by National Science Foundation grant number ACI-1053575

Supporting Information Available

Complete ITC binding curves and interaction data for nucleosides and oligonucleotides with nGO and reduced nGO, vacuum interaction energies from DFT calculations, thermodynamics of

nucleoside binding, kinetics of oligonucleotide desorption under constant force, salt effects at the single nucleoside level, rescaled LJ parameters, and force constants used in umbrella simulations. This information is available free of charge via the Internet at http://pubs.acs.org/.

Figures:

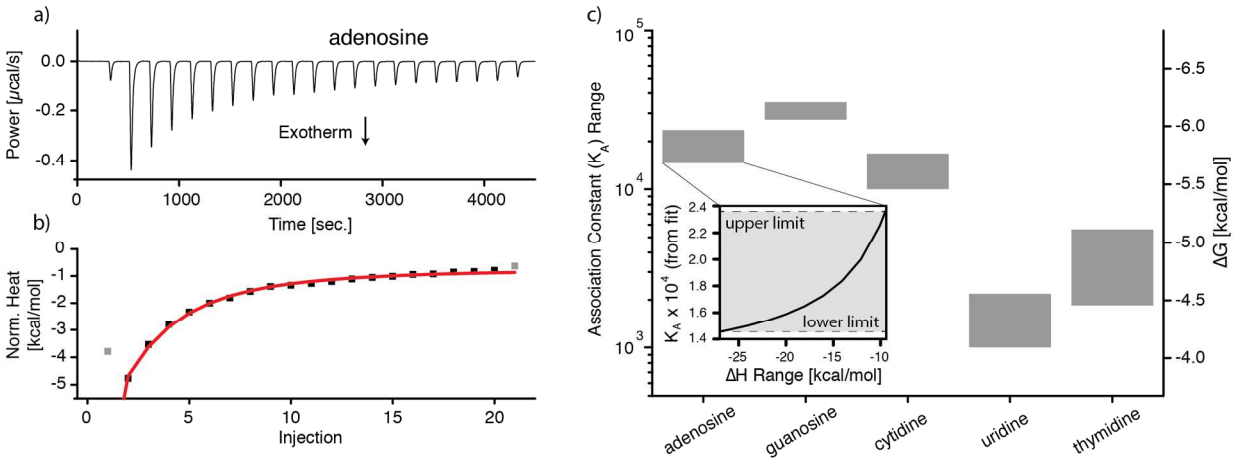

Figure 1: Experimental determination of graphene-nucleoside interactions a) Baseline corrected heat rate for a single Adenosine-nGO interaction experiment obtained with ITC, b) Normalized heat for each injection (squares) fit with a two state binding model with greyed data excluded, c) Upper and lower limits for the association constants based on enthalpy constrained fitting of mean ITC data from multiple data sets. The inset shows variation of the fit-determined association constant for adenosine while constraining enthalpy across the range of realistic values.

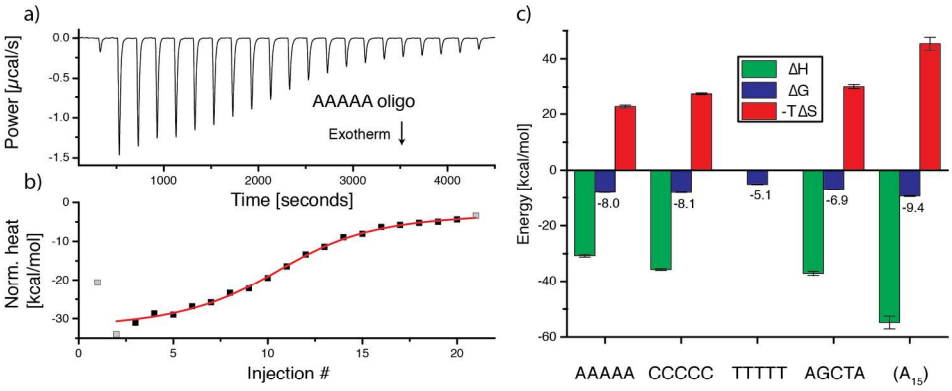

Figure 2: Experimental determination of graphene-oligonucleotide interactions. a) Baseline corrected heat rate for a 5mer poly adenosine oligonucleotide (A_5), b) Normalized heat for each injection (squares), fit with a two state binding model that excludes greyed data points, c) Determined interactions energies, with enthalpic and entropic decomposition for those with full binding curves.

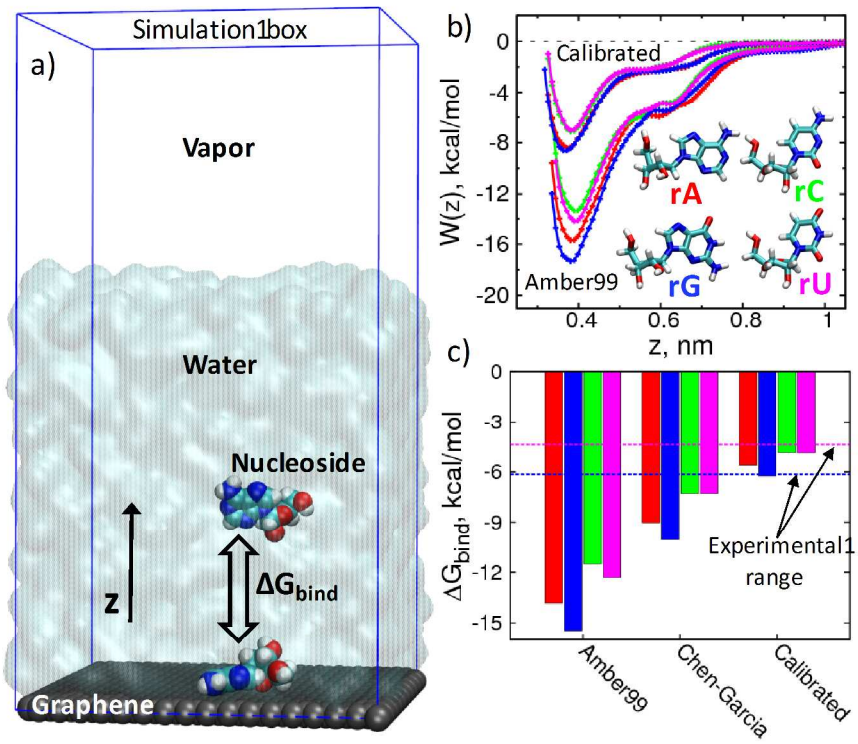

Figure 3. An experimentally calibrated molecular model for graphene-nucleic acid interactions: a) Schematic of the simulation box of the system. The graphene (black) and nucleic acid atoms are shown in space fill and water molecules are shown in a transparent gel representation. b) Potentials of mean force (PMFs) between single nucleoside and graphene calculated using Amber99 and calibrated (this work) parameters. c) Binding free energies of single nucleoside to graphene calculated from the PMFs from two existing force-fields and the one developed here. The range of experimental binding free energies of single nucleosides is shown using the dotted lines.

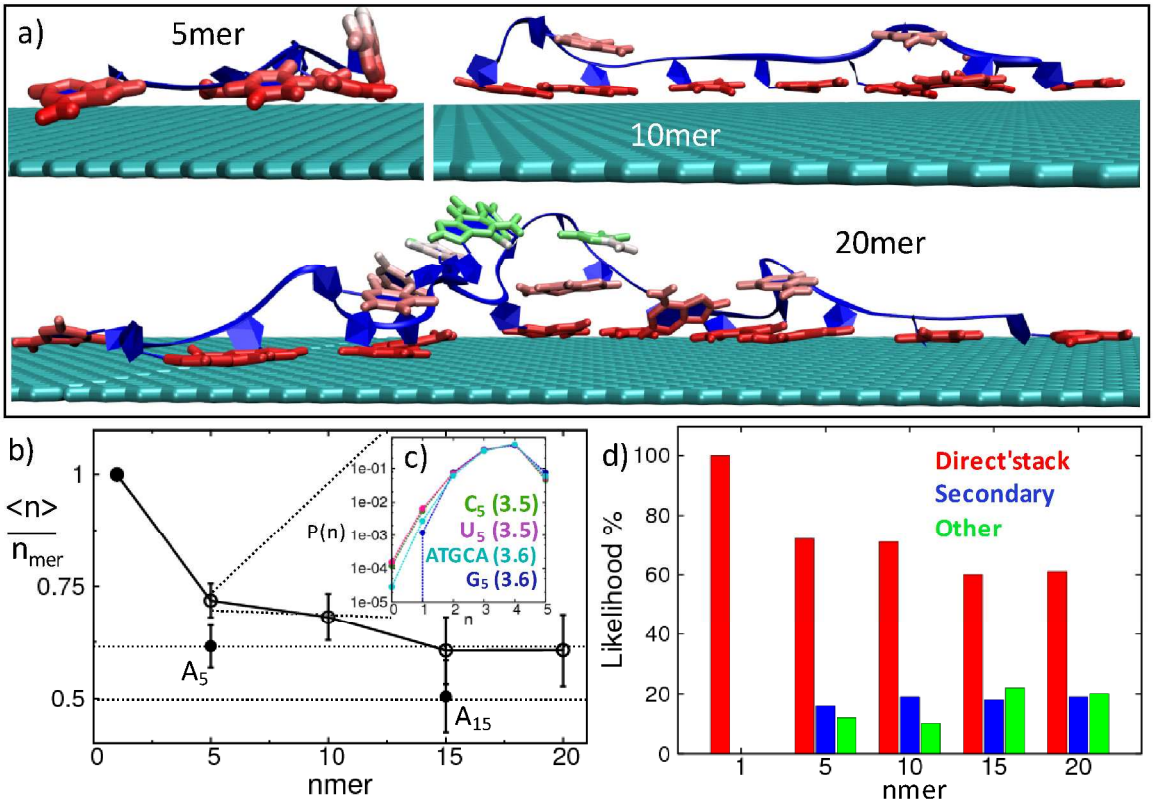

Figure 4. Structural characterization of oligos at the graphene interface: a) Simulation snapshots of the oligos (blue ribbons) at the graphene interface (cyan lattice). The bases are also shown in a licorice representation and colored according to their proximity to the graphene interface (red to white to green). b) Normalized average number of bases directly stacked on graphene for all the oligos. (open circles: Mixed sequence; closed circles: poly-A sequence) c) Probability distribution of number of bases stacked on graphene for various 5mer oligos (the average is shown in parentheses). d) Likelihood of observing the bases in direct or secondary stacked or non-stacked (other) conformations when bound to the graphene interface.

References

1. Geim, A. K.; Novoselov, K. S., The rise of graphene. *Nat. Mater.* **2007,** *6* (3), 183-91.
2. Novoselov, K. S.; Geim, A. K.; Morozov, S. V.; Jiang, D.; Zhang, Y.; Dubonos, S. V.; Grigorieva, I. V.; Firsov, A. A., Electric field effect in atomically thin carbon films. *Science* **2004,** *306* (5696), 666-9.
3. Balci, O.; Polat, E. O.; Kakenov, N.; Kocabas, C., Graphene-enabled electrically switchable radar-absorbing surfaces. *Nat. Commun.* **2015,** *6*, 6628.
4. Sydlik, S. A.; Jhunjhunwala, S.; Webber, M. J.; Anderson, D. G.; Langer, R., In vivo compatibility of graphene oxide with differing oxidation states. *ACS Nano* **2015,** *9* (4), 3866-74.
5. Zhu, A. Y.; Yi, F.; Reed, J. C.; Zhu, H.; Cubukcu, E., Optoelectromechanical multimodal biosensor with graphene active region. *Nano Lett.* **2014,** *14* (10), 5641-9.
6. Reed, J. C.; Zhu, A. Y.; Zhu, H.; Yi, F.; Cubukcu, E., Wavelength tunable microdisk cavity light source with a chemically enhanced MoS2 emitter. *Nano Lett.* **2015,** *15* (3), 1967-71.
7. Guo, Q.; Zhu, H.; Liu, F.; Zhu, A. Y.; Reed, J. C.; Yi, F.; Cubukcu, E., Silicon-on-Glass Graphene-Functionalized Leaky Cavity Mode Nanophotonic Biosensor. *ACS Photonics* **2014,** *1* (3), 221-227.
8. Chung, C.; Kim, Y. K.; Shin, D.; Ryoo, S. R.; Hong, B. H.; Min, D. H., Biomedical applications of graphene and graphene oxide. *Acc Chem Res* **2013,** *46* (10), 2211-24.
9. Zhang, Y.; Nayak, T. R.; Hong, H.; Cai, W., Graphene: a versatile nanoplatform for biomedical applications. *Nanoscale* **2012,** *4* (13), 3833-42.
10. Song, Y.; Qu, K.; Zhao, C.; Ren, J.; Qu, X., Graphene oxide: intrinsic peroxidase catalytic activity and its application to glucose detection. *Adv. Mater.* **2010,** *22* (19), 2206-10.
11. Wang, Y.; Li, Z.; Hu, D.; Lin, C. T.; Li, J.; Lin, Y., Aptamer/graphene oxide nanocomplex for in situ molecular probing in living cells. *J. Am. Chem. Soc.* **2010,** *132* (27), 9274-6.
12. Lu, C. H.; Yang, H. H.; Zhu, C. L.; Chen, X.; Chen, G. N., A graphene platform for sensing biomolecules. *Angew. Chem. Int. Ed. Engl.* **2009,** *48* (26), 4785-7.
13. Hizir, M. S.; Balcioglu, M.; Rana, M.; Robertson, N. M.; Yigit, M. V., Simultaneous detection of circulating oncomiRs from body fluids for prostate cancer staging using nanographene oxide. *ACS Appl. Mater Interfaces* **2014,** *6* (17), 14772-8.
14. Huang, P. J.; Liu, J., Molecular beacon lighting up on graphene oxide. *Anal. Chem.* **2012,** *84* (9), 4192-8.
15. Balcioglu, M., Buyukbekar, B. Z., Yavuz, M. S., & Yigit, M. V. (2014). Smart-polymer-functionalized graphene nanodevices for thermo-switch-controlled biodetection. *ACS Biomat. Sci. Eng.*, *1*(1), 27-36.
16. Liu, J., Adsorption of DNA onto gold nanoparticles and graphene oxide: surface science and applications. *Phys. Chem. Chem. Phys.* **2012,** *14* (30), 10485-96.
17. Robertson, N. M.; Salih Hizir, M.; Balcioglu, M.; Wang, R.; Yavuz, M. S.; Yumak, H.; Ozturk, B.; Sheng, J.; Yigit, M. V., Discriminating a Single Nucleotide Difference for Enhanced miRNA Detection Using Tunable Graphene and Oligonucleotide Nanodevices. *Langmuir* **2015,** *31* (36), 9943-52.

18. Robertson, N. M.; Hizir, M. S.; Balcioglu, M.; Rana, M.; Yumak, H.; Ecevit, O.; Yigit, M. V., Monitoring the multitask mechanism of DNase I activity using graphene nanoassemblies. *Bioconjug. Chem.* **2015,** *26* (4), 735-45.
19. Rana, M.; Balcioglu, M.; Robertson, N.; Yigit, M. V., Nano-graphene oxide as a novel platform for monitoring the effect of LNA modification on nucleic acid interactions. *Analyst* **2014,** *139* (4), 714-20.
20. Chehel Amirani, M.; & Tang, T., Binding of nucleobases with graphene and carbon nanotube: a review of computational studies. *J. Biomol. Struct. Dyn.* **2015**, *33*(7), 1567-1597.
21. Varghese, N.; Mogera, U.; Govindaraj, A.; Das, A.; Maiti, P. K.; Sood, A. K.; Rao, C. N., Binding of DNA nucleobases and nucleosides with graphene. *Chem. Phys. Chem.* **2009,** *10* (1), 206-10.
22. Das, A., Sood, A. K., Maiti, P. K., Das, M., Varadarajan, R., & Rao, C. N. R., Binding of nucleobases with single-walled carbon nanotubes: Theory and experiment. *Chem. Phys. Lett.* **2015**, *453*(4), 266-273.
23. Cavaluzzi, M. J.; Borer, P.N., Revised UV extinction coefficients for nucleoside-5'-monophosphates and unpaired DNA and RNA. *Nucleic Acids Research* **2004**, *32* (1), 13e–13.
24. Tellinghuisen, J., Calibration in isothermal titration calorimetry: heat and cell volume from heat of dilution of NaCl(aq), *Anal. Biochem.* **2007**, 360, 47–55.
25. Demarse, N.A.; Quinn, C.F.; Eggett, D.L.; Russell, D.J.; Hansen, L.D., Calibration of nanowatt isothermal titration calorimeters with overflow reaction vessels, *Anal. Biochem.* **2011**, 417, 247–255.
26. Kallansrud, G.; Ward, B., A comparison of measured and calculated single- and double-stranded oligodeoxynucleotide extinction coefficients. *Anal. Biochem.* **1996**, *236* (1), 134–138.
27. Antony, J.; Grimme, S., Structures and interaction energies of stacked graphene–nucleobase complexes. *Physical Chemistry Chemical Physics* **2008**, *10* (19), 2722-2729.
28. Kong, J.; White, C. A.; Krylov, A. I.; Sherrill, D.; Adamson, R. D.; Furlani, T. R.; Lee, M. S.; Lee, A. M.; Gwaltney, S. R.; Adams, T. R.; Ochsenfeld, C.; Gilbert, A. T. B.; Kedziora, G. S.; Rassolov, V. A.; Maurice, D. R.; Nair, N.; Shao, Y.; Besley, N. A.; Maslen, P. E.; Dombroski, J. P.; Daschel, H.; Zhang, W.; Korambath, P. P.; Baker, J.; Byrd, E. F. C.; Van Voorhis, T.; Oumi, M.; Hirata, S.; Hsu, C.-P.; Ishikawa, N.; Florian, J.; Warshel, A.; Johnson, B. G.; Gill, P. M. W.; Head–Gordon, M.; Pople, J. A., Q-Chem 2.0: A high-performance *ab initio* electronic structure program package. *J. Comp. Chem.* **2000**, 21, 1532–1548.
29. Rezác, J.; Kevin E. R.; Pavel H., S66: A well-balanced database of benchmark interaction energies relevant to biomolecular structures. *J. Chem. Theo. Comp.* **2011**, 7(8), 2427-2438.
30. Goerigk, L.; Holger K.; Grimme, S., Benchmarking Density Functional Methods against the S66 and S66x8 Datasets for Non-Covalent Interactions. *Chem. Phys. Chem.* **2011***,* 12(17), 3421-3433.
31. Hess, B.; Kutzner, C.; van der Spoel, D.; Lindahl, E., GROMACS 4: Algorithms for Highly Efficient, Load-Balanced, and Scalable Molecular Simulation. *J. Chem. Theo. Comp.* **2008**, 4(3), 435–447.

32. Bussi, G.; Donadio, D.; Parrinello, M., Canonical sampling through velocity rescaling. *J. Chem. Phys.* **2007**, 126, 014101-1--014101-7
33. Darden, T.; York, D.; Pedersen, L. Particle mesh Ewald - an N.LOG(N) method for Ewald sums in large systems. *J. Chem. Phys.* **1993**, 98, 10089−10092
34. Jorgensen W. L.; Chandrasekhar J.; Madura J. D.; Impey R. W.; Klein M. L., Comparison of simple potential functions for simulating liquid water. *J. Chem. Phys.* **1983,** 79(2), 926–935
35. Hess, B.; Bekker, H.; Berendsen, H.; Fraaije, J., LINCS: a linear constraint solver for molecular simulations. *J. Comp. Chem.* **1997**, 18, 1463−1472
36. Rosenbergl, J. M., The weighted histogram analysis method for free-energy calculations on biomolecules. I. The method. *J. Comp. Chem.* **1992***,* 13(8), 1011-1021
37. Stankovich, S.; Dikin, D. A.; Piner, R. D.; Kohlhaas, K. A.; Kleinhammes, A.; Jia, Y.; Wu, Y.; Nguyen, S. T.; Ruoff, R. S., Synthesis of graphene-based nanosheets via chemical reduction of exfoliated graphite oxide. *Carbon* **2007**, *45*(7), 1558-1565.
38. Cornell W. D.; Cieplak P.; Bayly C. I.; Gould I. R.; Merz K. M. Jr; Ferguson D. M.; Spellmeyer D. C.; Fox T.; Caldwell J. W.; Kollman P. A., A Second Generation Force Field for the Simulation of Proteins, Nucleic Acids, and Organic Molecules. *J. Am. Chem. Soc.* **1995**, 117, 5179–5197
39. Chen, A. A.; & García. A. E., High-resolution reversible folding of hyperstable RNA tetraloops using molecular dynamics simulations. *Proc. Natl. Acad. Sci.* **2013,** 110(42), 16820-16825.
40. He, Y.; Jiao, B.; Tang, H., Interaction of single-stranded DNA with graphene oxide: fluorescence study and its application for S1 nuclease detection. *RSC Advances* **2014**, 4(35), 18294-18300.
41. Liu, B.; Sun, Z.; Zhang, X.; Liu, J., Mechanisms of DNA sensing on graphene oxide. *Anal. Chem.* **2013**, *85*(16), 7987-7993.
42. Park, J. S.; Goo, N. I.; Kim, D. E., Mechanism of DNA adsorption and desorption on graphene oxide. *Langmuir* **2014**, *30*(42), 12587-12595.
43. Wu M.; Kempaiah R.; Huang P. J.; Maheshwari V.; Liu J., Adsorption and desorption of DNA on graphene oxide studied by fluorescently labeled oligonucleotides. *Langmuir* **2011** 27(6):2731-2738.

Table of Contents Figure: